Contents lists available at ScienceDirect

Arabian Journal of Chemistry

journal homepage: www.ksu.edu.sa

Palladium nanocubes-mediated Fenton catalysis combined with chloride ion-amplified electro-driven catalysis for dye degradation

Jingming Zhai [a,1], Heying Li [a,1], Shegan Gao [a,*], Hongbo Sun [b], Chuntao Zhao [b], Dongmei Yu [b], Xiantao Lin [c], Shaowen Cheng [c,*], Jinghua Li [a,b,c,**]

[a] The 1st Affiliated Hospital, School of Medical Technology and Engineering, Henan University of Science and Technology, Luoyang 471000, China
[b] Key Laboratory of Comprehensive and Highly Efficient Utilization of Salt Lake Resources, Qinghai Institute of Salt Lakes, Chinese Academy of Sciences, Qinghai Provincial Key Laboratory of Geology and Environment of Salt Lakes, Xining 810008, China
[c] The First Affiliated Hospital of Hainan Medical University, Key Laboratory of Hainan Trauma and Disaster Rescue, College of Emergency and Trauma, Hainan Medical University, Haikou 571199, China

ARTICLE INFO

Keywords:
Pd cubes
Electro-driven catalysis
Fenton catalysis
Synergistic degradation
MB

ABSTRACT

Electrochemical technology is frequently used to treat industrial dye wastewater. However, its degradation efficiency is restricted by pH, and the low current efficiency and high energy consumption limit its broader application. Based on this, we constructed an innovative electro-driven catalytic system by integrating nanotechnology with electric current. This system operates without pH constraints, has low energy consumption, and allows for the recycle and reuse of both electrodes and catalysts. Firstly, we synthesized palladium (Pd) cubes via a solvothermal method, and characterized their morphology, structural composition, and crystalline properties using transmission electron microscopy (TEM), energy dispersive X-ray spectroscopy (EDS), X-ray photoelectron spectroscopy (XPS), X-ray diffraction (XRD) and other methods. The prepared Pd cubes possessed dual catalytic properties of electro-driven catalysis and Fenton catalysis, achieving a synergistic degradation effect under an electric field. Subsequently, the study explored how catalysts dosage, H_2O_2 concentration, pH and Cl^- concentration affect the catalytic rate. The optimized system was able to degrade 99.17 % of MB within 1 h and was effective against various organic pollutants. After five cycles of reuse, the recovered catalysts maintained over 90 % degradation efficiency in decomposing MB. This process realizes efficient degradation with a low concentration of catalysts, offering a novel approach for nanotechnology in wastewater treatment under electro-driven conditions.

1. Introduction

As humanity entered the industrial era, the rapid development brought about a drastic deterioration of the natural environment. Water pollution from human activities, especially the significant discharge of dye wastewater from industries such as textiles, printing and dyeing, tanning, has emerged as a critical environmental concern. Most of this wastewater exhibits high chromaticity and is rich in organic pollutants. Even after treatment, it is still dissolved in solid form or suspended in aqueous solutions, which is typical difficult to degrade organic wastewater (Raja et al., 2024; Alharbi, 2024; Bukhari et al., 2024; Mutahir et al., 2024). Furthermore, these dyes often contain complex aromatic molecular structures, which makes them potentially highly toxic or teratogenic and difficult to biodegrade under normal conditions. If discharged directly into the ecosystem, it will not only severely pollute environments crucial for human survival, such as farmland and rivers, but will also pose a significant threat to human health (Liu and Wang, 2024; Zhang et al., 2024; Dursun, 2023). For instance, methylene blue (MB), a cationic phenothiazine dye widely used in fields such as dyes, textiles, and chemical indicators, has been classified as 3 carcinogen by the World Health Organization (WHO) (Ning et al., 2023; Fan et al., 2023; Yusuf et al., 2024). MB has severe adverse reactions on humans and animals, and is difficult to degrade completely. Therefore, it is crucial to develop methods that can effectively purify dye wastewater.

* Corresponding author.
** Corresponding author at: College of Medical Technology and Engineering, Henan University of Science and Technology, Luoyang 471000, China.
E-mail addresses: gsg112258@163.com (S. Gao), chengshaowen1@126.com (S. Cheng), anubiss1860@163.com (J. Li).
[1] These authors contributed equally to this work.

https://doi.org/10.1016/j.arabjc.2024.105851
Received 22 March 2024; Accepted 29 May 2024
Available online 31 May 2024

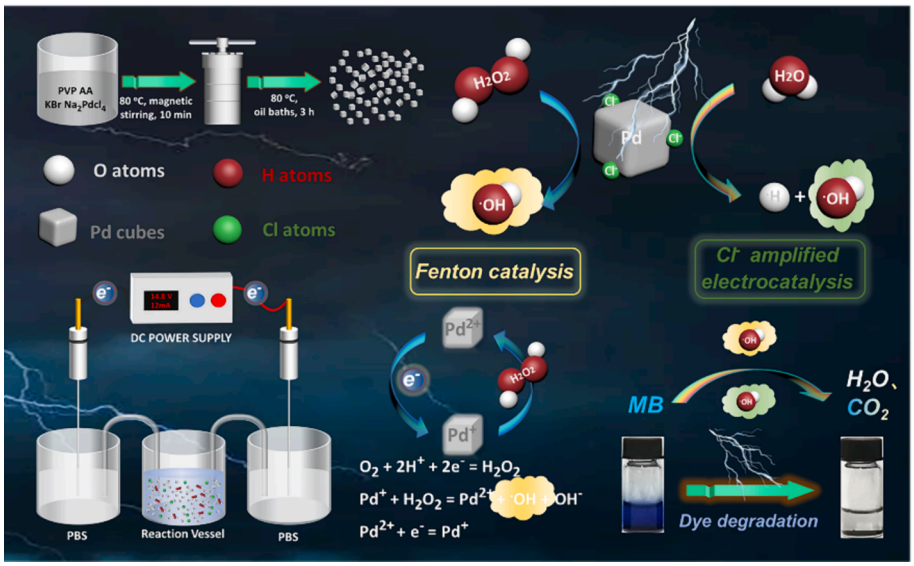

Scheme 1. Schematic mechanism of Pd cubes realizing electro-driven catalysis for synergistic Fenton catalytic degradation of MB dyes.

Currently, various methods for dye wastewater treatment including adsorption, flocculation, membrane separation, photocatalysis, Fenton catalysis, and electrochemical techniques have been exploited (Wang et al., 2024; Liu et al., 2024a; Tong et al., 2024; Lv et al., 2024; Liu et al., 2024b). Among them, electrochemical oxidation and Electro-Fenton (EF) as two types of electrochemical techniques, feature relatively simple equipment, small footprint, low operation and maintenance costs, effective prevention of secondary pollution, high controllability of reactions, and suitability for industrial automation, making them "environmentally friendly" techniques (Kareem et al., 2024; Xu et al., 2024). As a novel water treatment process, EF has been proven effective in discoloration and degradation of azo dyes in water. However, this technology needs to be operated within a limited pH range (2.0–3.5) and generates a considerable quantity of iron-rich sludge during the catalytic process (Lu et al., 2024; Song et al., 2024). Electrochemical oxidation has low current efficiency and high energy consumption, suitable only for treating organic wastewater with low concentration, which limits its further application and promotion (Santos et al., 2024; Yang et al., 2024).

In response to the aforementioned issue, previous researchers have proposed a novel concept of electrocatalytic technology by combining nanotechnology with electric current (Chen et al., 2021). Under an electric field, platinum nanoparticles (Pt NPs) adsorb chloride ions (Cl^-) and water molecules, leading to the occurrence of the Faraday cage effect on the surface of Pt NPs, creating hole doping conditions, followed by dissociation reaction of water molecules, which generates hydroxyl radicals (·OH) assisted by Cl^-. Previous studies have already demonstrated that metals such as Pt, Pd, and Ir exhibit electrocatalytic properties. However, current electrocatalytic research predominantly utilizes Pt NPs, with limited exploration into the application of Pd in electro-Fenton catalysis.

Concurrently, studies have indicated that Pd possesses peroxidase-like (POD) activity, and can undergo a catalytic activity similar to Fenton reaction with hydrogen peroxide (H_2O_2), resulting in the generation of •OH (Li et al., 2024; Xu et al., 2024; Kong et al., 2023; Qi et al., 2023). The superior electro-driven and Fenton catalytic performance of Pd cubes allows for the synergistically enhanced degradation of organic pollutants. This combined catalytic system features low energy consumption, easy control, and low cost. For example, using the piezoelectric material BiOCl, Wu et al. designed a synergistic piezo-photocatalytic system (Wu et al., 2024a; Wu et al., 2024b; Yu et al., 2024; Wu et al., 2023a; Wu et al., 2023b; Wu et al., 2023c; Wu et al., 2022a; Wu et al., 2022b; Wu et al., 2020; Li et al., 2024; Liu et al., 2023a; Liu et al., 2023b). The piezoelectric potential generated during the piezoelectric catalytic process addressed the issue of recombination of photogenerated carriers, thereby increasing the photocatalytic activity of BaOCl. Therefore, this efficient dye wastewater purification system designed by utilizing multiple catalytic properties of the catalysts, holds significant potential for application in dye degradation and wastewater treatment.

Inspired by this, we have synthesized single-atom Pd nanocubes using a simple one-step method, endowing them with multiple catalytic mechanisms and highly efficient dye contaminant degradation capabilities (Scheme 1). By applying low-voltage direct current (DC) in a double salt bridge system, Pd nanocubes can efficiently generate •OH under the electric field, and as Fenton-like catalysts, can induce the generation of •OH. This realizes the combination of electrocatalysis and Fenton catalysis to achieve efficient dye degradation. Furthermore, increasing the concentration of Cl^- in the electrolyte not only enhances the current intensity, but also improves the electro-driven catalytic performance, thereby increasing the production capacity of •OH. According to current understanding of the electrochemical techniques, this study offers a novel approach to enhancing the efficiency of electrocatalytic wastewater treatment and expands the further application of electrochemical wastewater treatment technologies.

2. Materials and methods

2.1. Materials

Sodium tetrachloropalladate (Na_2PdCl_4, 98 %), polyvinylpyrrolidone (PVP, MW≈55,000), potassium chloride (KCl, 99.8 %), sodium chloride (NaCl, ≥99.5 %), 3,3′,5,5′-tetramethylbenzidine (TMB), methylene blue (MB, ≥98.5 %), and hydrogen peroxide (H_2O_2, 30 %) were supplied by Aladdin (Shanghai, China). L-ascorbic acid (AA, 99.99 %) and potassium bromide (KBr, 99 %) were supplied by Macklin Biochemical Technology (Shanghai, China).

2.2. Synthesis of Pd cubes

Pd cubes were synthesized via a solvothermal method based on a previous study (Zhang et al., 2015; Chang et al., 2021). Firstly, PVP (105 mg), AA (60 mg), and KBr (600 mg) were dispersed in water (8 mL) and stirred magnetically under a water bath at 80 °C for 10 min. Subsequently, Na_2PdCl_4 (57 mg) was dissolved in water (3 mL) and added into the preheated solution, and then ultrasonication for 5 min. Finally,

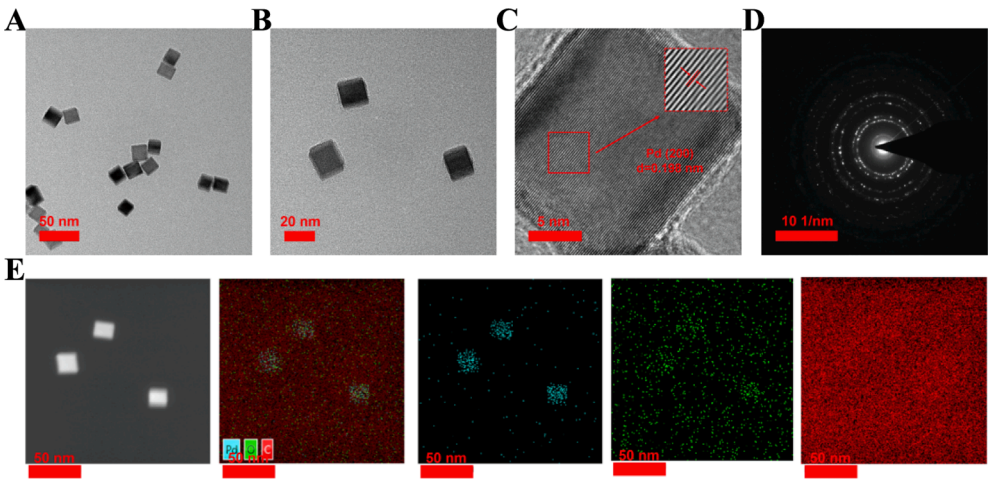

Fig. 1. Formation and characterization of Pd cubes. (A, B) TEM images. (C) HRTEM image. (D) SAED image. (E) EDS mapping image.

the mixed solution was transferred to a high pressure reactor and heated at 80 °C for 3 h. After cooling the solution to room temperature, the final product was collected by centrifugation at 11,000 rpm, washed twice with water and ethanol, dried in a vacuum freeze dryer, resulting in the formation of Pd nanocubes.

2.3. Characterization of Pd cubes

The morphology and elemental distribution of Pd nanocubes were characterized using field emission transmission electron microscopy (TEM, FEI Tecnai G2 F30, America, 300KV) and energy dispersive X-ray spectroscopy (EDS, FEI Tecnai G2 F30, America, 300KV). X-ray diffraction (XRD, Bruker D8-Advance, Germany, Cu Ka radiation l = 1.5406 Å) and X-ray photoelectron spectroscopy (XPS, Thermo escalab 250XI, America, C1s = 284.8 eV) were used to record the crystallographic information and surface chemical composition of Pd cubes. The UV–visible absorption spectrum of MB at room temperature was analyzed using a UV–visible spectrophotometer (NanoDrop One, Thermo Scientific, America). Electron paramagnetic resonance (EPR) spectroscopy were obtained using a Bruker EMXnano benchtop EPR spectrometer (Germany).

2.4. Fenton catalytic activity studies

To visualize and monitor the Fenton reaction activity of Pd cubes, TMB was chosen as a capture probe for·OH(Duan et al., 2024; Zhu et al., 2024; Zhu et al., 2024; Lin et al., 2024; Yang et al., 2024). Pd cubes (125 μg mL^{-1}) were placed in hydrochloric acid buffer solution (pH = 5) containing TMB (2 mM) and H_2O_2 (5 %). Within the specified reaction time, the absorption value and color change of oxTMB at 652 nm were measured and recorded by UV–visible spectrophotometer to determine the Fenton catalytic performance of Pd cubes for the generation of·OH.

2.5. Catalytic degradation experimrnts

Evaluate the electrocatalytic performance of Pd cubes by measuring the changes in MB absorbance during the catalytic decomposition of the dye. The electro-driven catalytic degradation process of MB is depicted in Figs. S4 and S5. 1 mL of PBS containing MB dye (100 μg mL^{-1}) was placed in a 24-well plate, fitted with Pt wire electrodes arranged symmetrically. Each well was connected via a salt bridge (Saturated KCl), and the two electrodes linked to the positive and negative terminals of a DC regulated power supply. By adding NaCl and H_2O_2 to the electrolyte cell, the impact of Cl^- concentration and the Fenton catalytic activity of Pd cubes on the degradation of MB were examined.

The absorbance of different concentrations of MB at 664 nm was measured to establish a calibration curve relating MB concentration to absorbance. In the catalytic experiments, 5 μL of the reaction solution was pipetted at specific time intervals, and the absorbance of the mixture was measured using a UV–visible spectrophotometer to monitor the degradation of MB. Each catalytic degradation experiment was repeated at least three times to minimize random errors. The catalytic degradation efficiency of MB was calculated according to Eq. (1).

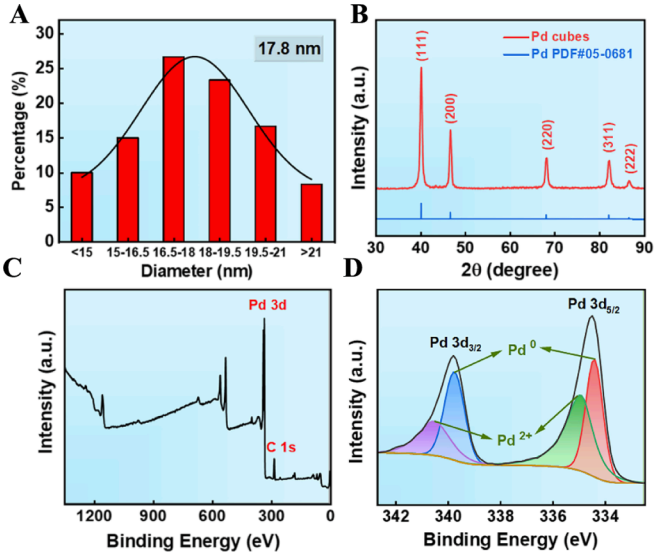

Fig. 2. Representation of Pd cubes. (A) Particle size distribution curve of Pd cubes. (B) XRD pattern. (C, D) XPS analysis.

$$\text{MB Removal efficiency}\,(\%) = \frac{(C0 - Ct)}{C0} \times 100\% \quad (1)$$

In this formula, C_0 and C_t represent the initial concentration (μg mL^{-1}) of MB and the residual concentration after t min of degradation, respectively.

3. Results and discussion

3.1. Preparation and characterization of Pd cubes

In this study, Na_2PdCl_4 was employed as the precursor of Pd ions, and PVP and AA were serving as both surfactants and reducing agents to regulate the size and shape of Pd NPs. The solvothermal method was utilized to dissolve the Pd salts and surfactants, followed by the Pd ions

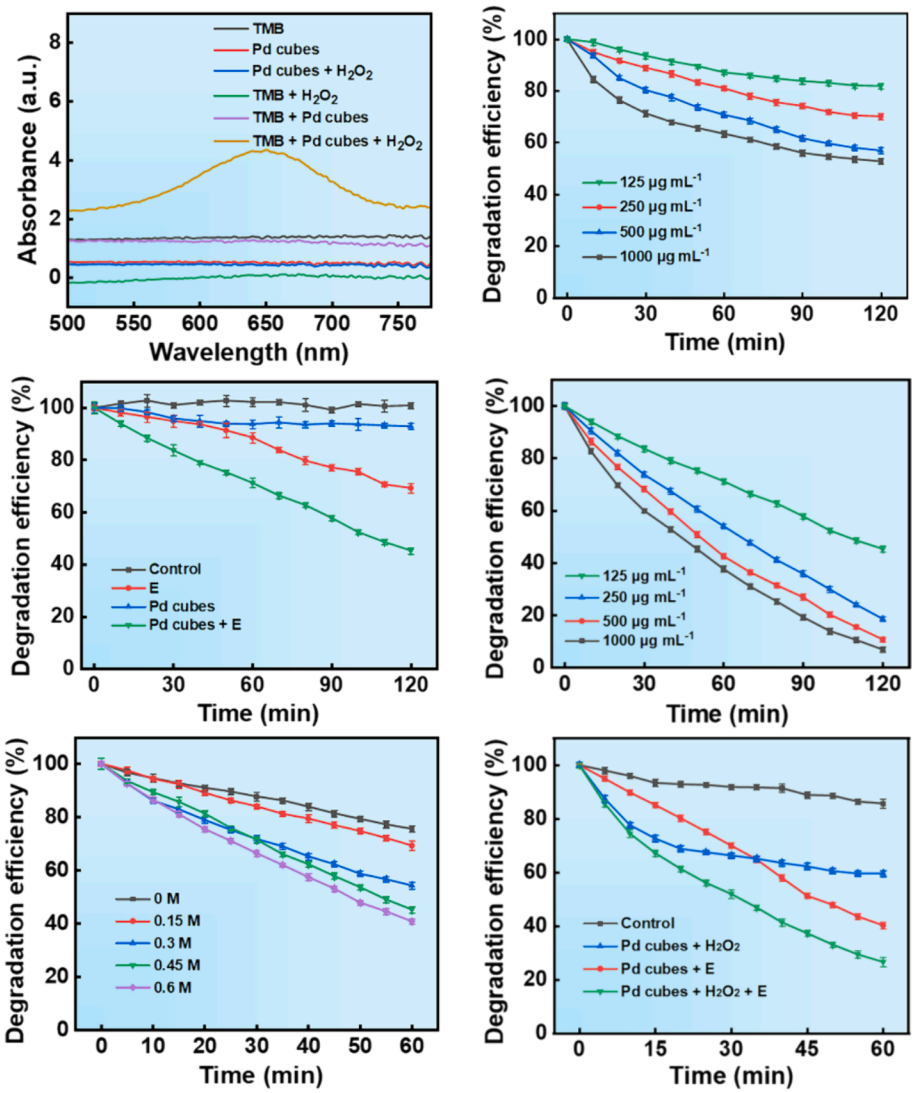

Fig. 3. Degradation efficiency of MB by Pd cubes. (A) UV–vis absorption spectrum of TMB under different conditions (Concentration of Pd cubes: 125 μg mL^{-1}, H_2O_2: 1.25 %, TMB: 200 mM). (B) Effect of different concentrations of Pd cubes as Fenton catalysts on MB degradation efficiency (Concentration of H_2O_2: 1.25 %, MB: 100 mg/L). (C) Degradation efficiency of MB under different control groups (Concentration of Pd cubes: 125 μg mL^{-1}, MB: 100 mg/L, Cl^-: 0.6 M). (D) Efficiency of electro-driven catalytic degradation of MB at different concentrations of Pd cubes (Concentration of MB: 100 mg/L, Cl^-: 0.6 M). (E) Degradation efficiency of MB at different concentrations of Cl^- (Concentration of Pd cubes: 1000 μg mL^{-1}, MB: 100 mg/L). (F) Degradation efficiency of MB under different catalytic systems (Concentration of Pd cubes: 1000 μg mL^{-1}, H_2O_2: 1.25 %, MB: 100 mg/L, Cl^-: 0.6 M).

were rapidly nucleated and formed into Pd cubes under high temperature and high pressure conditions. Scanning electron microscopy (SEM) and transmission electron microscopy (TEM) images (Fig. 1A, B, Fig. S1) revealed uniformly sized cubic structures of Pd NPs, and its average particle size was 17.8 nm (Fig. 2A). High-resolution transmission electron microscopy (HRTEM) and selected area electron diffraction (SAED) results demonstrated the highly single crystal structure of Pd cubes, and the lattice stripe spacing measured 0.198 nm, aligning with the (200) crystal plane of Pd cubes (Fig. 1C, D). Energy dispersive X-ray spectroscopy (EDS) spectra detected Pd and O signals uniformly distributed on the surface of Pd cubes, as expected (Fig. 1E).

X-ray diffraction (XRD) tests comprehensively examined the crystalline nature of Pd cubes. As shown in Fig. 2B, five typical diffraction peaks appeared at 40.154°, 46.684°, 68.105°, 82.177°, and 86.582°, aligning with the (111), (200), (220), (311), and (222) crystal planes of Pd (PDF#05-0681). X-ray photoelectron spectroscopy (XPS) analysis confirmed the elemental composition, chemical states and electronic structure of Pd cubes. As depicted in Fig. 2C, Pd cubes contained Pd and C elements, consistent with EDS results. The XPS results exhibited 334.5 eV and 339.8 eV two primary peaks, attributed to the Pd 3d5/2 and Pd 3d7/2 orbitals (Fig. 2D), which is consistent with previous findings (Ming et al., 2020; Fang et al., 2018). The peak fitting of the Pd 3d orbitals has revealed the presence of multivalent Pd, facilitating the cycling of Pd^0/Pd^+ to Pd^{2+} and enabling the generation of·OH via Fenton catalytic reaction. These all provide essential conditions for the oxidative degradation of MB.

3.2. Catalytic degradation performance analysis

The degradation efficiency of Pd cubes as electro-driven catalysis/Fenton catalysts for organic pollutants was evaluated using MB as the representative. Initially, the Fenton-like catalytic activity of Pd cubes was assessed using a TMB chromogenic probe. TMB can be converted to the oxidized state of TMB (oxTMB) by·OH, exhibiting a distinctive absorption peak at 652 nm. Upon addition of Pd cubes to a TMB and H_2O_2 solution (pH = 5), the solution turned deep blue, and the absorption value at 652 nm increased (Fig. 3A, Fig. S2), indicating that Pd cubes can induce·OH generation by reacting with H_2O_2 as a Fenton-like reagent.

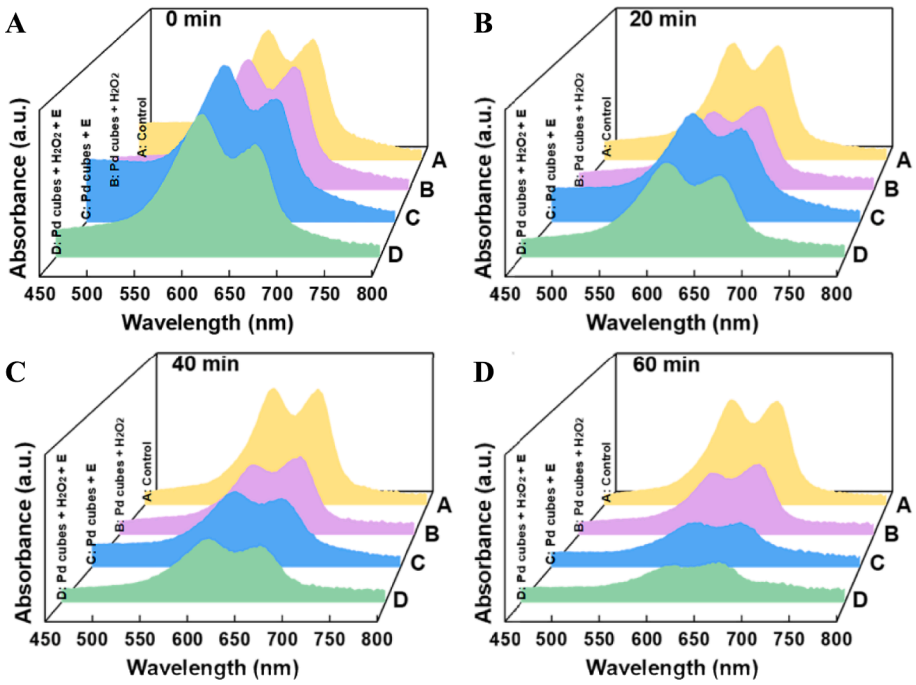

Fig. 4. UV–vis absorption spectrum of MB in four catalytic degradation systems at different moments. (A-D) UV–vis absorption spectrum at 0, 20, 40, and 60 min.

We plotted the standard concentration-absorbance curve of MB in the scope of 0–100 mg/L (Fig. S3) and calculated the degradation efficiency of MB based on the equation of this curve ($A_{(absorbance)} = 0.04522C_{(concentration)} + 0.77507$, $R^2 = 0.99322$). We studied the impact of Pd cubes concentration on the degradation rate (Fig. 3B), and discovered that increasing the concentration of the Fenton catalysts from 125 μg mL^{-1} to 1000 μg mL^{-1} significantly enhanced the degradation efficiency of MB, but the degradation effect was still insignificant as it could only be degraded by 47.21 % within 2 h.

Electro-driven catalytic degradation is an efficient method that combines electrochemistry with nanotechnology, possesses unique advantages compared to traditional electrochemical oxidation methods. To elucidate the electro-driven catalytic performance of Pd cubes, we constructed a double salt bridge system (Figs. S4 and S5) and controlled the catalytic reaction process through the switch of a DC regulated power supply. Compared to other sample groups, Pd cubes exhibited the most intense catalytic degradation of MB under the electric field (Fig. 3C). To further investigate the optimum reaction conditions for degrading MB, we examined the influence of Pd cubes concentration on the catalytic reaction. As Pd cubes concentration increased, the

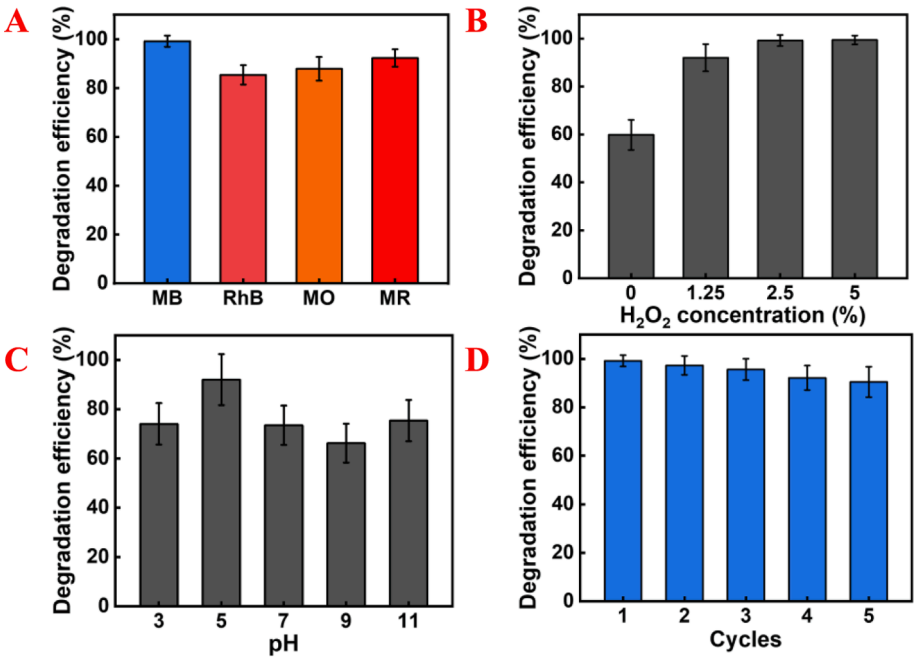

Fig. 5. The effect of reaction conditions on the degradation efficiency of MB by Pd cubes (Concentration of Pd cubes: 1000 μg mL^{-1}, MB: 100 mg/L, Cl^-: 0.6 M). (A) pH value (Concentration of H_2O_2: 1.25 %). (B) H_2O_2 concentration (pH = 5). (C) Degradation of dye contaminant (Concentration of H_2O_2: 2.5 %, pH = 5). (D) Reuse of Pd cubes for dye degradation (Concentration of H_2O_2: 2.5 %, pH = 5).

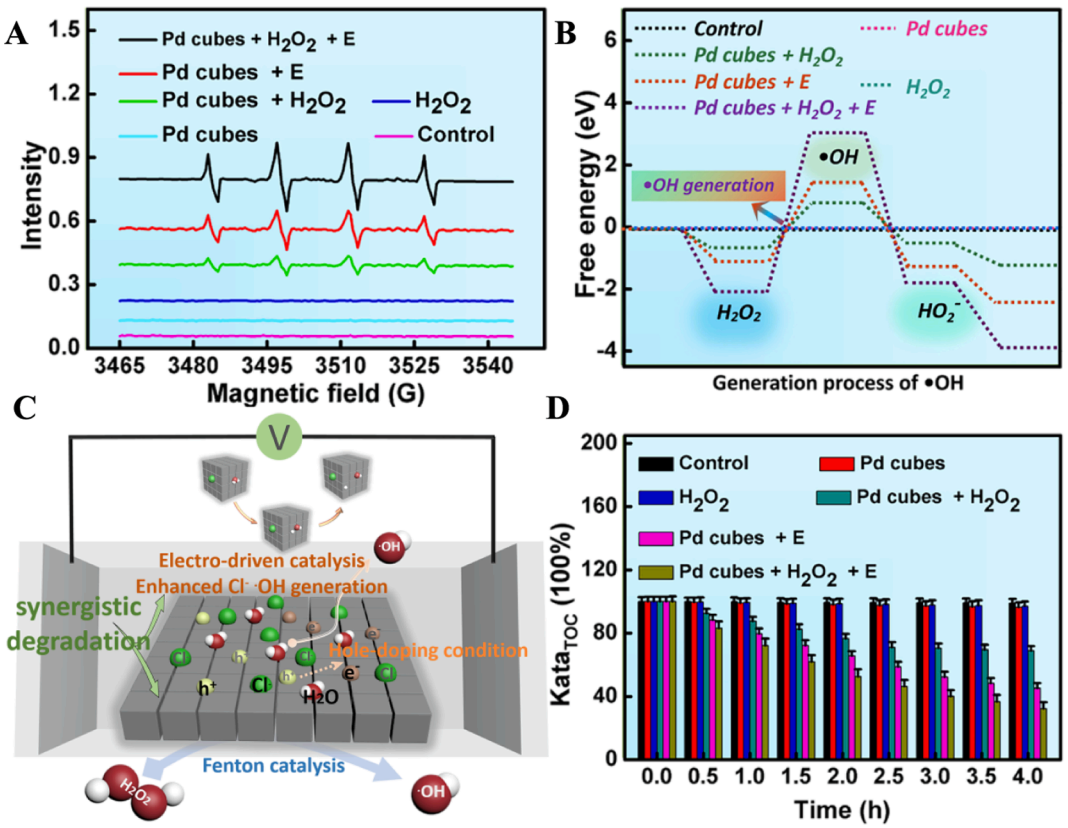

Fig. 6. Catalytic degradation mechanism of MB by Pd cubes. (A) EPR spetra. (B) DFT calculation. (C) Schematic representation of the combined degradation of Pd cubes. (D) TOC removal rate of MB aqueous solution.

degradation rate of MB accelerated, requiring only 2 h to approach complete degradation (Fig. 3D, Fig. S6).

By exploring the mechanism of electric current-triggered·OH production by Pd cubes, we discovered that the presence of Cl^- in the electrolytic cell is crucial for electro-driven catalytic degradation (Fig. 6C). Under the same DC, in the absence of Cl^-, MB degradation triggered by Pd cubes was significantly slower, whereas with increasing Cl^- concentration, the degradation rate of MB markedly accelerated (Fig. 3E). This may be attributed to Cl^- favorably adsorbing on the face-centered cubic (Fcc) sites on the (1 1 1) surface of Pd cubes and acting as the primary driving force under the surface current of Pd cubes to promote the dissociation of water molecules, thereby generating highly oxidative·OH, which is consistent with previous research results.

Under the electric field, we added H_2O_2 to the reaction vessel and found that its addition significantly accelerated the catalytic degradation efficiency of MB. This is because H_2O_2 can undergo Fenton catalytic reaction with Pd cubes in the electrolytic cell, which promoted the accumulation of·OH in the electro-driven catalytic system, thereby achieving synergistic degradation effect of Fenton catalysis and electro-driven catalysis. The degradation rates of MB (Fig. 3F) and the UV–visible absorption spectrum (Fig. 4A–D) in each reaction system within 60 min were recorded, and observations revealed that the degradation rate within the first 30 min was notably higher in the Fenton catalysis system compared to the electro-driven catalysis system. As H_2O_2 was gradually consumed, the degradation capacity peaked, in contrast, the degradation rate of MB in the electro-driven catalysis system remained relatively stable and surpassed that of the Fenton catalysis system at 60 min. The combined degradation capability of Pd cubes enabled the MB to be degraded by 73.41 % in 60 min, rendering the dye nearly colorless, which was significantly higher than the degradation rates observed in other sample groups (Fig. S7).

The limited applicable pH range has been a major bottleneck for both electrochemical and Fenton catalytic reactions. To overcome this, we explored how the initial pH affects MB degradation. Fig. 5A showed that approximately 70 % of MB can be quickly eliminated across the pH range of 3–11. This broad pH window removes the need for pH adjustment in conventional catalytic reactions, thereby lowering the cost consumption of the catalytic system·H_2O_2 concentration is a crucial factor influencing the Fenton catalytic reaction, so we examined the effect of varying H_2O_2 concentration on the degradation rate. Increasing H_2O_2 concentration from 1.25 % to 2.5 % results in the degradation of 99.17 %, similar to the efficiency of the system with 5 % H_2O_2 (Fig. 5B). Thus, considering the cost of practical application, the optimal H_2O_2 concentration in our Pd-based catalytic system is 2.5 %.

Fig. 5C further assessed the degradation ability of Pd cubes on various organic pollutants. Remarkably, the optimized system achieved degradation rates of 99.17 % for MB, 85.39 % for rhodamine B (RhB), 87.85 % for methyl orange (MO), and 92.28 % for methyl red (MR) within 60 min. These findings demonstrated the applicability of the electro-driven/Fenton catalytic system for removing organic pollutants degradation, thereby increasing its potential for practical application.

The recyclability of the catalysts is essential for treating industrial dye wastewater. Therefore, we recovered the used Pd cubes and assessed their reusability through cyclic stability test. As shown in Fig. 5D, even after five cycles, the degradation efficiency remained above 90 %, demonstrating the excellent recyclability of Pd cubes. In addition, we compared the degradation efficiency of Pd cubes with previous related catalytic systems, further demonstrating its potential as an efficient catalyst for the degradation of organic pollutants (Table S1) (Zhang et al., 2023; Chen et al., 2024). The slight reduction in MB degradation efficiency may be due to the loss of catalytic sites caused by the leaching of Pd ions. After five cycles, the leaching rate of Pd ions remained low, and with the total release of about 0.09484 %.

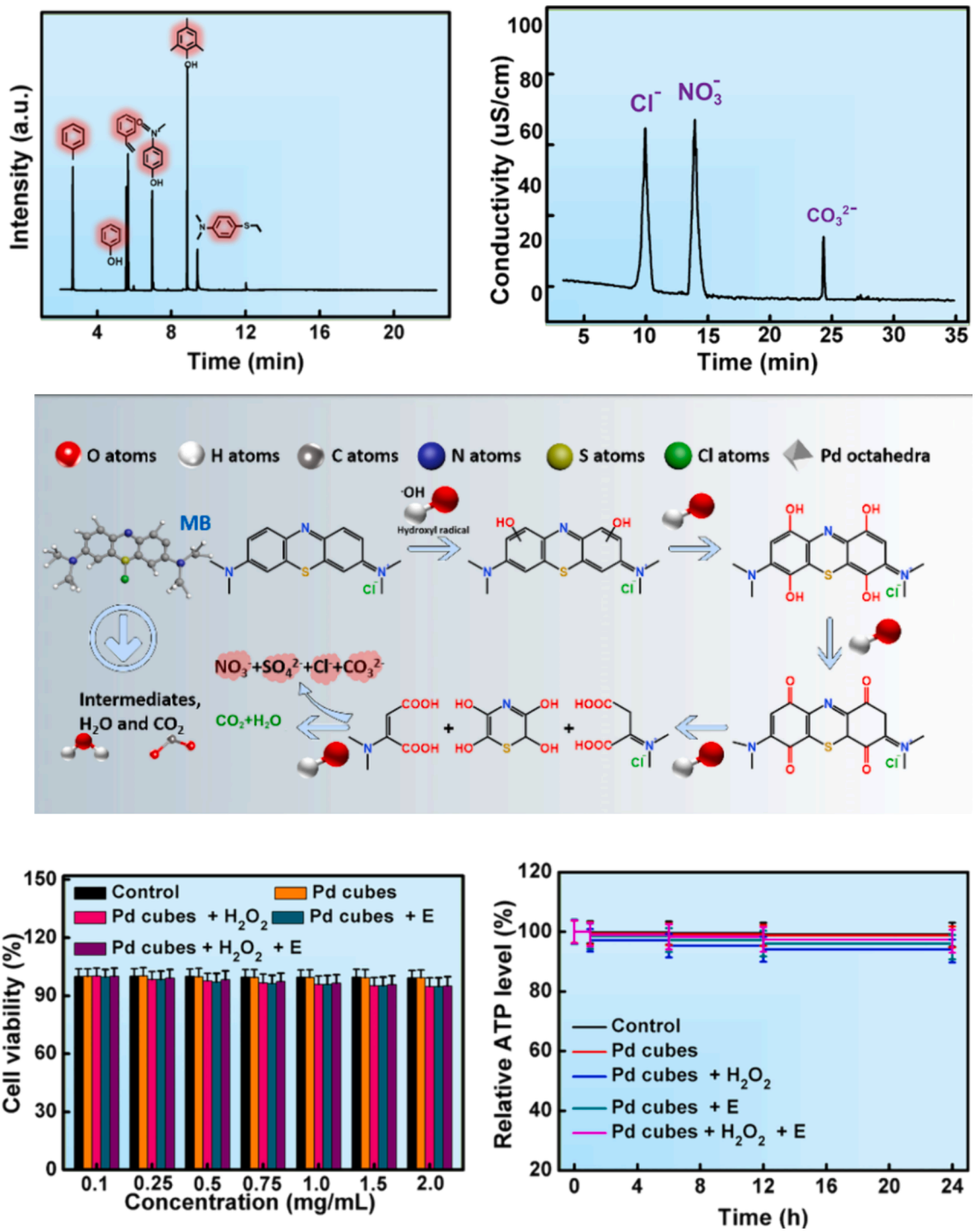

Fig. 7. The decomposition process of MB. (A, B) GC–MS and IC test results during the degradation of MB. (C) Degradation pathway of MB. (D, E) Cell viability and ATP activity after co-incubation with Pd cubes.

3.3. Catalytic degradation mechanism investigations

To explore the catalytic degradation mechanism, 5,5-Dimethyl-1-pyrroline N-oxide (DMPO) was employed as a trapping agent to monitor the catalytic reaction in the system. Electron paramagnetic resonance (EPR) spectroscopy results (Fig. 6A) revealed that the characteristic peaks of 1:2:2:1 appeared in the other three groups compared with the control group, indicating that Pd cubes served as an effective electro-driven catalysis/Fenton catalysts for inducing the generation of·OH. Furthermore, compared with the individual Fenton catalysis or electrocatalysis system, the combined catalytic degradation system exhibited the strongest·OH signals, confirming the dual catalytic capability of Pd cubes. Using density functional theory (DFT) to estimate the energy of·OH, and the results turned out that the combined catalysis system exhibited the strongest energy signals of·OH, which was consistent with the EPR spectroscopy results (Fig. 6B).

Building upon the aforementioned findings, we have revealed a possible catalytic degradation mechanism. As illustrated in Fig. 6C, under the action of the electric field, Cl^- and water molecules were adsorbed on the (1 1 1) surface of Pd cubes, inducing the Faraday cage

effect on the surface of Pd cubes, leading to a hole doping condition. Subsequently, the charge between the water molecules and Pd cubes began to transfer, and the charge gradually accumulated on Pd atoms near oxygen atoms. With the increase in hole doping concentration, the charge on hydrogen atoms decreased more pronounced. Simultaneously, the length of the H-O bond increased, leading to the dissociation of water molecules and the formation of·OH. Additionally, Pd cubes as the effective Fenton catalysts, can react with H_2O_2 to generate·OH, which enhances the catalytic capability of Pd cubes. Ultimately, the formed·OH attacked the MB molecules, and under the potent oxidation effect of·OH, MB molecules were gradually decomposed.Total Organic Carbon (TOC) is a crucial indicator for assessing organic pollution in water. Its determination has become a primary method for water quality monitoring and quality control worldwide, and was widely applied in areas such as drinking water and wastewater treatment. Hence, we measured the residual amount of organic pollutants in water ($Kata_{TOC}$) according to Eq. (2) to evaluate the degradation efficiency of the catalysts.

$$\mathrm{KataTOC}\,(100\%) = \frac{\mathrm{TOCt}}{\mathrm{TOC0}} \times 100\% \quad (2)$$

where TOC_0 represents the total amount of TOC in the water, and TOC_t represents the carbon content of the remaining organic matter in the water after degradation for t (h). As shown in Fig. 6D, the total organic carbon removal rate reached 70.2 % after continuous degradation of low-concentration MB dye solution for 4 h. This process realizes efficient mineralization of organic pollutants in water and demonstrates promising potential for industrial treatment of organic pollution.

Subsequently, gas chromatography-mass spectrometry (GC–MS) and ion chromatography (IC) were utilized to analyze the intermediates and the final products formed during the degradation of MB. Fig. 7A and B revealed the presence of volatile organic small molecules such as toluene, phenol, styrene, 2,4,6-trimethylphenol, as well as ionic compounds such as Cl^-, NO_3^-, SO_4^{2-}, and CO_3^{2-} during the decomposition process of MB. Therefore, Fig. 7C proposed a possible degradation pathway for MB. Pd cubes exhibited their dual catalytic capability to generate·OH, and the highly oxidative·OH oxidized and broke the C=C bonds, opening the benzene ring, gradually and decomposing the organic macromolecules into small molecular compounds, ultimately mineralizing them into CO_2 and H_2O.

An ideal wastewater treatment technology should possess characteristics such as high efficiency, energy efficient, good recyclability, and good biocompatibility. The nanocatalysts used in wastewater treatment should be safe, non-toxic, green, and should not cause secondary pollution to water. The cell toxicity of the catalysts was evaluated by MTT method, where NRK-52E cells were co-incubated with Pd cubes for 24 h to evaluate their viability. The results showed that even at elevated concentration of Pd cubes (2 mg/L), cell viability and ATP activity remained above 95 %, indicating excellent biocompatibility of Pd cubes (Fig. 7D, E). Therefore, Pd cubes are harmless to microorganisms in water and will not disrupt the balance of ecosystem in the process of wastewater treatment, and have extensive application prospects in the field of wastewater treatment.

4. Conclusion

In conclusion, a straightforward and efficient technique has been devised to fabricate Pd nanocubes. Utilizing the synergistic effect of electro-driven and Fenton catalysis of Pd cubes, we achieved the decomposition of organic pollutants in wastewater. The impact of Pd cubes concentration, Cl^- concentration, H_2O_2 concentration, and pH on degradation efficiency was systematically studied. The optimized Pd cubes + H_2O_2 + E system exhibited excellent performance, degrading 99 % of MB within 60 min. Due to multiple catalytic properties and low metal leaching rate, Pd cubes demonstrated outstanding cycling performance, maintaining over 90 % MB degradation efficiency even after five cycles. This research offered valuable insights into designing and developing synergistic catalytic systems, and could inspire further research on efficient catalysts with multiple catalytic activities for dye degradation and environmental remediation.

CRediT authorship contribution statement

Jingming Zhai: Data curation, Conceptualization. **Heying Li:** Writing – original draft. **Shegan Gao:** Writing – review & editing, Resources. **Hongbo Sun:** Formal analysis, Data curation. **Chuntao Zhao:** Methodology, Investigation. **Dongmei Yu:** Validation, Supervision. **Xiantao Lin:** Visualization. **Shaowen Cheng:** Writing – review & editing, Investigation. **Jinghua Li:** Writing – review & editing, Project administration.

Declaration of competing interest

The authors declare that they have no known competing financial interests or personal relationships that could have appeared to influence the work reported in this paper.

Acknowledgement

This research received funding from several sources, including the National Natural Science Foundation of China (Grant Nos. 32260237, U20A2088, and 82260373), the Innovation Scientists and Technicians Troop Construction Projects of Henan Province (Grant No. 21HASTIT046), the Top Young Talents in Central Plains (Grant No. ZYQNBJRC2021-02), the Natural Science Foundation of Hainan Province (Grant No. 823MS045), the Key Scientific Research Project of Henan Province Universities (Grant No. 22A320033), the Innovation Team Foundation of Qinghai Office of Science and Technology (2022-ZJ-903) and the Second Tibetan Plateau Scientific Expedition and Research Program (Grant NO.2019QZKK0805-02).

Appendix A. Supplementary data

Supplementary data to this article can be found online at https://doi.org/10.1016/j.arabjc.2024.105851.

References

Alharbi, K.H., 2024. Efficient removal of methylene blue from aqueous solutions using mixed oxides of cobalt oxide and tungsten trioxide modified graphene oxide. J. Saudi Chem. Soc. 28 (1), 101802.
Bukhari, S.A.S., Zafar, M., Mazhar, F., Ahmed, A., Fazal, T., Rehman, F., Razzaq, A., Kim, W.Y., 2024. Development of nickel doped graphitic carbon nitride (GCN) photocatalyst for enhanced degradation of textile pollutant under visible light irradiation. J. Saudi Chem. Soc. 28 (2), 101801.
Chang, M., Hou, Z., Wang, M., Yang, C., Wang, R., Li, F., Liu, D., Peng, T., Li, C., Lin, J., 2021. Single-atom Pd nanozyme for ferroptosis-boosted mild-temperature photothermal therapy. Angew. Chem. Int. Ed. 60 (23), 12971–12979.
Chen, T., Han, G., Li, X., 2021. Platinum–copper alloy nanoparticles armored with chloride ion transporter to promote electro-driven tumor inhibition. Bioact. Mater. 12, 143–152.
Chen, M., Zhang, J., Guo, P., Zhai, J., Liu, X., Yu, D., You, X., Li, J., 2024. PdPtCu nanoflower mediated photothermal enhanced Fenton catalysis for recyclable degradation of methylene blue. Inorg. Chem. Commun. 160, 111841.
Duan, N., Chang, Y., Su, T., Zhang, X., Lu, M., Wang, Z., Wu, S., 2024. Generation of a specific aptamer for accurate detection of sarafloxacin based on fluorescent/colorimetric/SERS triple-readout sensor. Biosens. Bioelectron. 249, 116022.
Dursun, S., 2023. Removal of cationic dye pollutants from wastewater with HS loaded semi-IPN composites: kinetic and thermodynamic studies. Environ. Monit. Assess. 196 (1), 27.
Fan, L., Zhu, H., Wang, K., Liu, H., Hu, W., Xu, X., Yan, S., 2023. Study on the degradation of methylene blue by Cu-doped SnSe. Molecules 28 (16), 5988.
Fang, C., Zhao, J., Jiang, R., Wang, J., Zhao, G., Geng, B., 2018. Engineering of hollow PdPt nanocrystals via reduction kinetic control for their superior electrocatalytic performances. ACS Appl. Mater. Interfaces 10 (35), 29543–29551.
Kareem, Thenmozhi, K., Hari, S., Ponnusamy, V.K., Senthilkumar, S., 2024. Metal-free carbon-based anode for electrochemical degradation of tetracycline and metronidazole in wastewater. Chemosphere 351, 141219.

Kong, L., Chen, D., Zhang, X., Zhou, L., Deng, Y., Wei, S., 2023. Controllable fabrication of Hg–Pd–PdO heterostructures as efficient peroxidase mimics for carcinoembryonic antigen detection. ACS Appl. Nano Mater. 6 (5), 3618–3626.

R. Li, W. Zhao, Z. Han, N. Feng, T. Wu, H. Xiong, W. Jiang, Self-cascade nanozyme reactor as a cuproptosis inducer synergistic inhibition of cellular respiration boosting radioimmunotherapy, Small (2024) e2306263.

Li, X., Liu, H., Zhang, Y., Mahlknecht, J., Wang, C., 2024. A review of metallurgical slags as catalysts in advanced oxidation processes for removal of refractory organic pollutants in wastewater. J. Environ. Manage. 352, 120051.

Lin, Z., Dong, T., Niu, L., Zhang, X., Wang, M., Liu, X., Cai, Y., Liu, A., 2024. Mechanism of ferrous ions reversibly inhibiting of oxidase-Like activity of Co_3O_4 nanowires and its application in horticultural fertilizer analysis. Chem. Eng. J. 482, 148775.

Liu, G., Fei, H., Feng, Z., Shao, Q., Zhao, T., Guo, W., Li, F., 2024b. Tri-phase interface to enhance the performance of piezoelectric photocatalysis and recyclability of hydrophobic BiOI/$BaTiO_3$ heterojunction. J. Clean. Prod. 440, 140886.

Liu, H., Li, X., Zhang, X., Coulon, F., Wang, C., 2023b. Harnessing the power of natural minerals: A comprehensive review of their application as heterogeneous catalysts in advanced oxidation processes for organic pollutant degradation. Chemosphere 337, 139404.

Liu, X., Wang, J., 2024. Decolorization and degradation of various dyes and dye-containing wastewater treatment by electron beam radiation technology: an overview. Chemosphere 351, 141255.

Liu, G., Zhang, X., Liu, H., He, Z., Show, P.L., Vasseghian, Y., Wang, C., 2023a. Biochar/layered double hydroxides composites as catalysts for treatment of organic wastewater by advanced oxidation processes: a review. Environ. Res. 234, 116534.

Liu, S., Zhang, J., Theliander, A., Chen, W., Wu, J., Wu, L., 2024a. Construction of self-repairing polyethersulfone membrane with high density hydrophilic microregions by two dimensional restricted channels for enhanced dyes/salts selective separation. Environ. Res. 247, 118266.

Lu, Y., Feng, M., Wang, Y., 2024. Enhancing the heterogeneous electro-Fenton degradation of methylene blue using sludge-derived biochar-loaded nano zero-valent iron. J. Water Process Eng. 59, 104980.

Lv, Z., Liu, H., Zhao, J., Wang, R., Xie, T., Qi, Y., Yu, Y., Lv, X., Sun, S., 2024. Temperature and photosensitive PVDF-g-PNIPAAm/GPE-PDA@ZnO composite membranes with efficient dyes separation capability and light-cleaning function. Eur. Polym. J. 206, 112780.

Ming, J., Zhu, T., Yang, W., Shi, Y., Huang, D., Li, J., Xiang, S., Wang, J., Chen, X., Zheng, N., 2020. Pd@Pt-GOx/HA as a novel enzymatic cascade nanoreactor for high-efficiency starving-enhanced chemodynamic cancer therapy. ACS Appl. Mater. Interfaces 12 (46), 51249–51262.

Mutahir, S., Khan, M.A., Qunhui, Y., Mehboob, S., Bououdina, M., Elkholi, S.M., Khan, A., Abumousa, R.A., Humayun, M., 2024. MOF-derived ZnO/g-C_3N_4 nanophotocatalyst for efficient degradation of organic pollutant. J. Saudi Chem. Soc. 28 (2), 101821.

Ning, R., Kim, S., Sun, E., Jiang, Y., Baek, J., Li, Y., Robinson, A., Vallez, L., Zheng, X., 2023. Enhanced H_2O_2 upcycling into hydroxyl radicals with GO/Ni:FeOOH-coated silicon nanowire photocatalysts for wastewater treatment. Nano Lett. 23 (14), 6323–6329.

Qi, W., Song, M., Wang, M., Yu, H., 2023. Designing M13 bacteriophage and Fe-nanonest self-assembly system for universal and facile preparation of metal single atoms as stable mimicking enzymes. ACS Nano 17 (24), 25483–25495.

Raja, R.I., Rashid, K.T., Toma, M.A., AbdulRazak, A.A., Shehab, M.A., Hernadi, K., 2024. A novel Polyethersulfone/Chamomile (PES/Chm) mixed matrix membranes for wastewater treatment applications. J. Saudi Chem. Soc. 28 (2), 101805.

Santos, A.J.D., Shen, H., Lanza, M.R.V., Li, Q., Garcia-Segura, S., 2024. Electrochemical oxidation of surfactants as an essential step to enable greywater reuse. Environ. Technol. Innov. 34, 103563.

Song, G., Zheng, Y., Zhou, M., 2024. The electro-Fenton/sulfite process with Fe-Mn bimetallic catalyst for diclofenac degradation at neutral pH. J. Environ. Chem. Eng. 12 (2), 112299.

Tong, Y., Wu, Y., Xu, Z., Luo, L., Jia, R., Han, R., Xu, S., 2024. Hydrolysis co-deposition of bio-inspired hybrid hydrophilic network antifouling loose nanofiltration membrane for effective dye/salt separation. J. Membr. Sci. 694, 122444.

Wang, M., Yan, R., Shan, M., Liu, S., Tang, H., 2024. Fabrication of crown ether-containing copolymer porous membrane and their enhanced adsorption performance for cationic dyes: experimental and DFT investigations. Chemosphere 352, 141363.

Wu, Z., Luo, W., Zhang, H., Jia, Y., 2020. Strong pyro-catalysis of shape-controllable bismuth oxychloride nanomaterial for wastewater remediation. Appl. Surf. Sci. 513, 145630.

Wu, Z., Wu, S., Hong, S., Shi, X., Guo, D., Zhang, Y., Xu, X., Chen, Z., Jia, Y., 2022a. Lead-free $Bi_{0.5}Na_{0.5}TiO_3$ ferroelectric nanomaterials for pyro-catalysis dye pollutant removal under cold–hot alternation. Nanomaterials 12 (22), 4091.

Wu, Z., Xu, T., Ruan, L., Guan, J., Huang, S., Dong, X., Li, H., Jia, Y., 2022b. Strong tribocatalytic nitrogen fixation of graphite carbon nitride g-C_3N_4 through harvesting friction energy. Nanomaterials 12 (12), 1981.

Wu, Z., Xu, T., Wang, X., Zhang, L., Zhao, C., Wu, W., Zhu, G., Jia, Y., 2023a. Natural tourmaline for pyroelectric dye decomposition under 25–60 ℃ room-temperature cold-hot fluctuation. Sep. Purif. Technol. 327, 124971.

Wu, Z., Fan, B., Zhang, L., Yao, Y., Hong, S., Yu, H., Jia, Y., 2023b. Strongly enhanced piezoelectric-catalysis of $ZnSnO_3$/graphite hybrid materials for dye wastewater decomposition. Ceram. Int. 49 (18), 29614–29621.

Wu, Z., Shi, X., Liu, T., Xu, X., Yu, H., Zhang, Y., Qin, L., Dong, X., Jia, Y., 2023c. Remarkable pyro-catalysis of g-C_3N_4 nanosheets for dye decoloration under room-temperature cold-hot cycle excitation. Nanomateials 13 (6), 1124.

Wu, Z., Zhu, Z., Ma, J., Zhou, M., Wu, Z., You, H., Zhang, H., Li, N., Wang, F., 2024a. High piezo-photocatalysis of $BaTiO_3$ nanofibers for organic dye decomposition. Surf. Interfaces 48, 104308.

Wu, Z., Xu, T., Zhang, L., Liu, T., Wu, Z., Zhu, G., Jia, Y., 2024b. Ferroelectric $BaTiO_3$/Pr_2O_3 heterojunction harvesting room-temperature cold-hot alternation energy for efficiently pyrocatalytic dye decomposition. J. Adv. Ceram. 13 (1), 44–52.

Xu, H., Sun, X., Yang, H., Cui, J., Wang, J., Kang, Y., Deng, J., Huang, G., 2024. Degradation of aqueous phenol by combined ultraviolet and electrochemical oxidation treatment. J. Clean. Prod. 436, 140672.

Xu, X., Zhang, J., Wang, X., Fang, H., Shi, S., Wu, F., Zhou, N., Shen, J., Sun, B., 2024. Multifunctional Pd single-atom nanozyme for enhanced cascade chemodynamic therapy of chronic wounds. ACS Appl. Nano Mater. 7 (3), 3445–3457.

Yang, Y., Xu, J., Zhou, R., Qin, Z., Liao, C., Shi, S., Chen, Y., Guo, Y., Zhang, S., 2024. Coordinated carbon dots-Fe featuring synergistically enhanced peroxidase-like activity at neutral pH for specific and background-free detection of dichlorvos. Carbon 219, 118831.

Yang, C., Zhao, W., Wang, Z., Guo, R., Shao, D., Xu, H., Yan, W., Song, H., 2024. New hierarchical Ti/SnO_2-PbO_2/CNT electrode: enhanced electrochemical properties and improved electrochemical oxidation towards various real wastewaters. J. Water Process Eng. 58, 104889.

Yu, H., Wei, X., Wang, M., Zhang, Y., Wu, Z., Guo, F., Han, J., 2024. Macroscopic polarization enhancement boosting piezo-photocatalytic performance via Nb-doping on B-site of $Bi4Ti_3O_{12}$ nanosheets. J. Adv. Ceram. 13 (4), 437–446.

Yusuf, L.A., Ertekin, Z., Fletcher, S., Symes, M.D., 2024. Enhanced ultrasonic degradation of methylene blue using a catalyst-free dual-frequency treatment. Ultrason. Sonochem. 103, 106792.

Zhang, J., Lei, K., Cheng, J., Luo, L., Liu, X., Li, J., 2023. Sea urchin-like PdCuAu nanoclusters mediated photothermal enhanced Fenton catalysis for degradation of dye pollutants. J. Alloy. Compd. 958, 170494.

Zhang, L., Roling, L.T., Wang, X., Vara, M., Chi, M., Liu, J., Choi, S.-I., Park, J., Herron, J. A., Xie, Z., Mavrikakis, M., Xia, Y., 2015. Platinum-based nanocages with subnanometer-thick walls and well-defined, controllable facets. Science 349 (6246), 412–416.

Zhang, H., Xue, K., Wang, B., Ren, W., Sun, D., Shao, C., Sun, R., 2024. Advances in lignin-based biosorbents for sustainable wastewater treatment. Bioresour. Technol. 395, 130347.

Zhu, X., Feng, T., Chen, Y., Xiao, Y., Wen, W., Wang, S., Wang, D., Zhang, X., Liang, J., Xiong, H., 2024. Reactive oxygen-correlated photothermal imaging of smart COF nanoreactors for monitoring chemodynamic sterilization and promoting wound healing. Small e2310247.

Zhu, X., Li, H., Hou, S., Song, P., Zheng, J., Wu, T., Zhao, H., Liu, Q., 2024. A novel three-stage continuous sensing platform for H_2O_2 and cholesterol based on $CuFeS_2$ nanozyme: theoretical calculation and experimental verification. Chem. Eng. J. 482, 148589.